sciendo

ACTA CHEMICA IASI, **26_2**, 281-306 (2018)

DOI: 10.2478/achi-2018-0018

SURFACE MODIFICATION OF OLIVE STONE WASTE FOR ENHANCED SORPTION PROPERTIES OF CADMIUM AND LEAD IONS

Mahmoud Belalia[a*], Meriem Bendjelloul[b], Abdallah Aziz[c] and El Hadj Elandaloussi[b]

[a]*Laboratoire SEA2M, Université Abdelhamid Ibn Badis, 27000 Mostaganem, Algerie*
[b]*Laboratoire ESNVTA, Centre Universitaire Ahmed Zabana, 48000 Relizane, Algerie*
[c]*Laboratoire de Valorisation des Matériaux, Université Abdelhamid Ibn Badis, 27000 Mostaganem, Algerie*

Abstract: This paper reports the synthesis and characterization of an efficient anionic olive stone waste-based material as new ion-exchanger adsorbent. The olive stone waste was subjected to an alkaline pretreatment in order to enhance their reactivity towards maleic anhydride. The maleate-derived material MOS was characterized by FTIR, ^{13}C NMR, TGA and DSC. The resulting sodium form of material NaMOS was subjected to batch experiments in order to evaluate its cadmium and lead removal efficiency. Adsorption experimental data showed a uniform and rapid process. Both Langmuir and Freundlich isotherm models were found to fit adequately the equilibrium isotherm data. The sorption capacities reached 240.96 mg Cd g^{-1} and 127.38 mg Pb g^{-1}. The thermodynamic parameters showed that the process was exothermic and the adsorption occurred spontaneously. The desorption experiments show a quantitative recovery of the metal ions from NaMOS material.

Keywords: olive stone waste; alkaline treatment; functionalization; sorption; metal removal; regeneration.

* Mahmoud Belalia, *e-mail*: mahmoud.belalia@univ-mosta.dz

Introduction

Owing to their non-degradable, persistent and accumulative nature, heavy metals are toxic even in trace amounts, being a source of environmental concern.[1-2] Cadmium and lead are discharged from various industries such as storage batteries, textile, pigment, plastic, electroplating, metallurgical processes and mine drainage.[3] Therefore, in order to remove the heavy metals from wastewaters, several processes have been developed including chemical precipitation,[4] solvent extraction,[5] ion exchange on resins[6-8] and so on. However, these methodologies face some limitations as they become less effective for the treatment of high volumes of effluents and low metal concentrations. In addition, they can also create sludge disposal problem or hazardous sub-products. [9-10]

During the last decades, efforts were made to develop effective and inexpensive adsorbents, as: activated carbon,[11-14] natural zeolites,[15-17] aquatic plants-based sorbents[18-19] and solid phase extraction[20] for wastewater treatment. It is now recognized that the removal of heavy metals using low-cost adsorbents derived from agricultural waste is an effective and economic process for water treatment. Thus, a wide variety of agricultural waste materials such as sawdust,[21] bagasse fly ash[2,22] rice husk[23], banana peels[24] have been used as low-cost alternatives to expensive adsorbents.

Agricultural waste represents an abundant, inexpensive, and readily available source of renewable lignocellulosic biomass. The agricultural sector of Algeria annually produces large amounts of olive fruit and their industrial processing equally generates tons of whole stones. Chemical modification of lignocellulosic waste is an attractive approach for the enhancement of their metal removal capacity. The chemical composition of

olive stone waste consists mainly of lignin, cellulose and hemicelluloses.[25] The hydroxyl groups from the surface are the most abundant and reactive sites of the material which can be used for the incorporation of a variety of functional groups. In an anterior work, we successfully incorporated succinyle linkers into the lignocellulosic matrix of olive stone waste where the carboxylate end groups of the spacer showed excellent removal capacity of cadmium ions from aqueous solutions, with a maximum uptake capacity of 200 mg g^{-1}.[26] The free rotation of sp^3 carbons along the succinate spacer allows the bending of the terminal carboxylate groups over the matrix which may reduce the overall uptake capacity. This study examines the concept of substituting succinate by a maleate spacer on the lignocellulosic waste. Such a linker having a double bond of cis configuration will necessarily lead to a *syn* adduct after ring opening and where the unsaturation should prevent the free rotation. Moreover, the proximity of the two carbonyl groups within the spacer may also play a cooperative part in chelating metal ions.

However, in our attempts to achieve effective functionalization of the lignocellulosic matrix of raw olive stone waste through esterification reaction with maleic anhydride, we encountered difficulties in getting adducts with fair degree of substitution. The presence of multiple functional groups in the lignocellulosic material complicates the chemical reaction course, and the functionalization was substantially limited. Therefore, in order to overcome these limitations and prior to the esterification reaction with maleic anhydride, we envisaged to subject the raw olive stone waste to an alkaline treatment to further enhance the reactivity of hydroxyl groups.

Herein, we report the successful functionalization of the alkali pretreated olive stones waste with maleic anhydride by esterification in heterogeneous basic conditions. The as-prepared sorbent material was

subsequently charged with sodium and evaluated in the removal of cadmium and lead ions in aqueous solutions. Sorption kinetics, isotherms, effects of pH and temperature have been investigated to identify a sorption mechanism of Cd(II) and Pb(II). The high performance of maleate-derived olive stone waste after regeneration cycles has been carefully examined to ascertain its stability and reusability. Finally, the great efficiency of the maleate-containing sorbent material in water remediation was clearly demonstrated.

Results and discussion

Characterization

The FTIR spectrum of raw olive stone waste HO–OS (Figure 1) illustrates the complex chemical composition of raw olive stone waste and revealed active functional groups such as carbonyl and hydroxyl groups of the lignocellulosic material which may interact with heavy metal ions throughout the adsorption process.[27-28] A glance at the NaO–OS spectrum reveals the disappearance of the absorption band at 1740 cm^{-1} occurring in the spectrum of the precursor HO–OS. This band is characteristic for the carbonyl functions of carboxylic acid, aldehyde and esters groups attributed to lignin. This result clearly indicates that alkaline treatment with 20 wt.% NaOH determines the complete removal of all extractable substances, tannins, pectin, and hemicelluloses in a single step and the solubilization of a quite significant part of lignin.

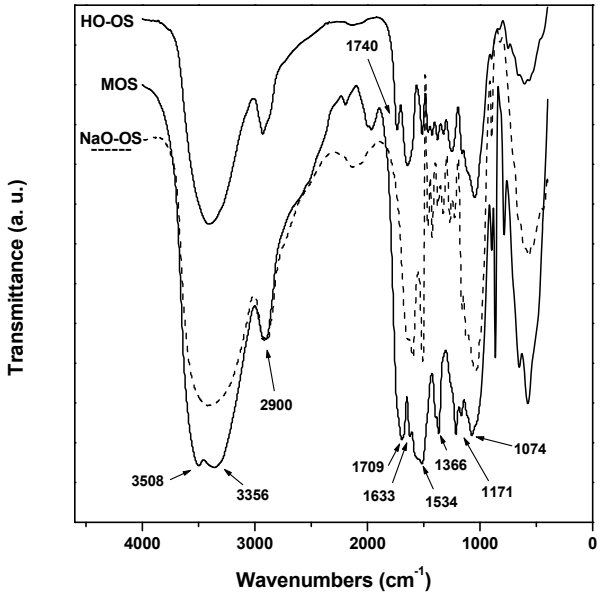

Figure 1. FTIR spectra of raw olive stone waste (HO-OS), alkaline treated waste NaO-OS and maleated olive stone (MOS).

The esterification/ring opening of NaO-OS by the maleic anhydride was successful, in the spectrum of MOS a strong overlapped absorption band centered at 1709 cm^{-1} appears, due to the synergistic absorption of carbonyl bonds of both ester and carboxylate anion groups from the maleate spacer. Besides this absorption band, the spectrum shows the intensities of two absorption bands at 1633 and 1171 cm^{-1} attributed to C=C bond and to the C–O stretching in the esters, respectively.[29-30]

The solid state CP-MAS ^{13}C NMR spectra of HO-OS, NaO-OS and MOS are shown in Figure 2. The spectrum of HO-OS exhibits signals at 105, 89, 82, 72, 63 and 55 ppm assignable to the carbon atoms from cellulose, and broad signals of low intensities assigned around 140-180 ppm, characteristic for lignin carbon. Moreover, the signal from 20.7 ppm is assigned to the methyl of the acetyl groups in hemicelluloses. It is worth

highlighting that the alkaline treatment of HO-OS leads to a material nearly free of lignin and hemicelluloses, as shown in NaO-OS ^{13}C spectrum.

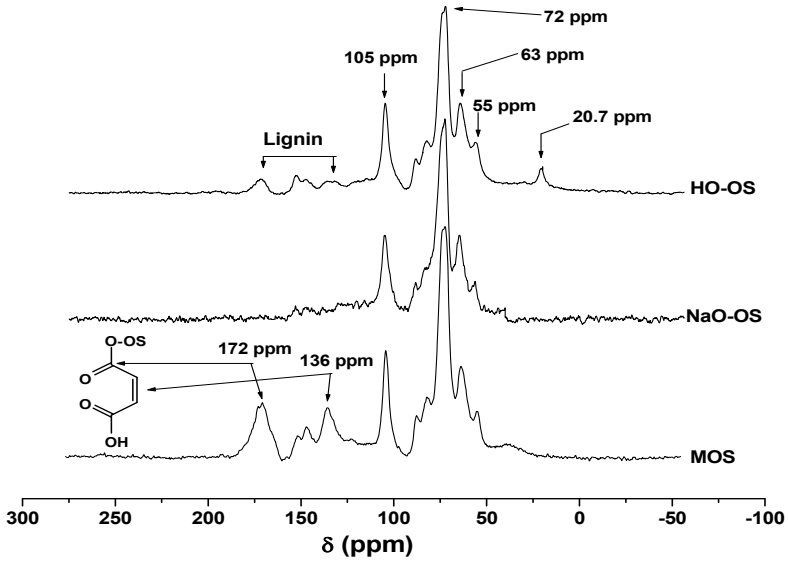

Figure 2. Solid state CPMAS ^{13}C NMR spectra of HO-OS, NaO-OS and MOS.

On the other hand, the analysis of MOS spectrum emphasizes the esterification of NaO-OS with maleic anhydride by the emergence of two additional intense signals centered at 172 and 136 ppm attributed to carbon atoms of carbonyl C=O (ester and carboxylic acid) and C=C (vinyl), respectively, from maleate group. Likewise, the presence of carboxylic acid groups is suggested by the pH_{zpc} value (4.5), which indicates the acid character of the material. Furthermore, the titration of carboxylic acid groups gave a CEC value of 2.8 mequiv. g^{-1}. These results are in good agreement with the strong intensities of signals attributed to the maleate groups observed in FTIR and MAS ^{13}C NMR spectra of MOS.

The BET surface area of SO-ONa and MOS were found to be 5.0398 and 4.4813 m^2/g, respectively. The decrease of the surface area is most likely due to packing brought by the maleic group of atoms, thereby hindering the access of nitrogen molecules to the surface.

The thermogravimetric analysis (TGA) of NaO-OS and MOS samples (Figure 3) indicates that the functionalization of olive stone waste with maleic linkers enhanced the thermal stability of MOS material, NaO-OS was degraded at lower temperatures than MOS. Indeed, the onset temperature of active pyrolysis of NaO-OS is 220°C, whereas the maleated olive stone waste MOS begins to decompose at 243°C. On the other hand, the temperatures for 50% weight loss are 315°C (NaO-OS) and 378°C (MOS).

On the differential scanning calorimetry analysis (DSC) (Figure 4), the onset of decomposition of the chemically modified olive stone waste (MOS) is at 287°C. Other exothermic peaks show up at 435°C before the reaction with maleic anhydride and at 740°C after the reaction, corresponding to the cellulose decomposition.

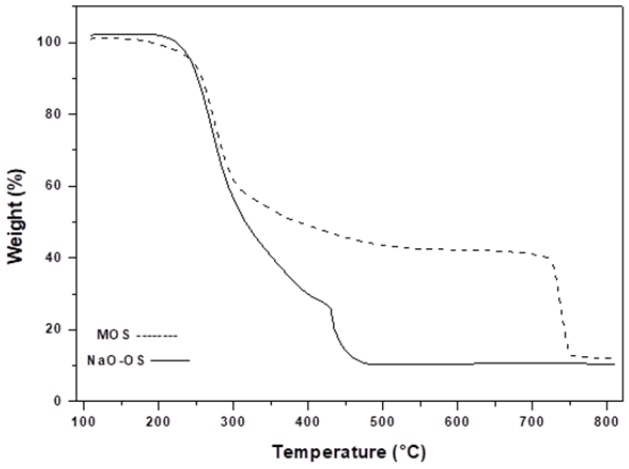

Figure 3. TGA analysis of NaO-OS and MOS.

These observations showed that esterification with maleic anhydride leads to a material with a higher stability.

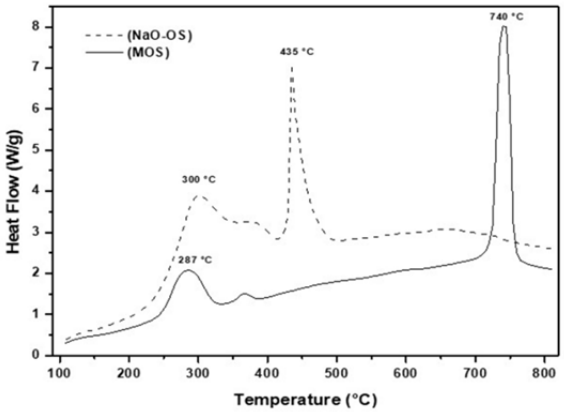

Figure 4. DSC analysis of NaO-OS and MOS.

Effect of pH

The pH of the solution is a key factor when the impact of metal sorption on pH variation is followed. Taking into account the base character of NaMOS used as adsorbent, the influence of pH was examined at target pH values set between 4 and 6, to prevent the adsorbent protonation and the metal precipitation. Previous similar work on adsorbents with carboxylate groups revealed that the metal sorption is insignificant at low pH values[26, 31]. In fact, the base properties of NaMOS induce proton binding, leading to the conversion of NaMOS into acid MOS. Figure 5 shows the influence of pH on Pb(II) and Cd(II) sorption onto NaMOS. The sorption capacity progressively increases up to pH 5 and tends to stabilize beyond this value. Based on these results, the pH value was set to pH 5 for the study of sorption isotherms and uptake kinetics.

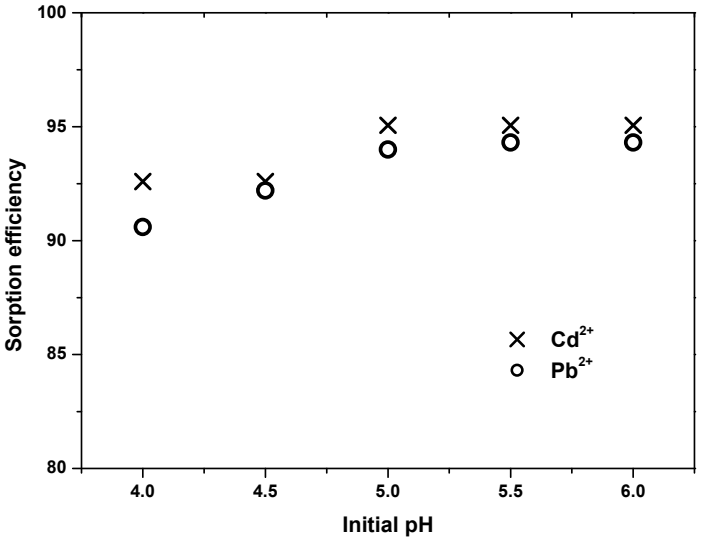

Figure 5. Effect of pH on the removal of Cd^{2+} and Pb^{2+} by NaMOS

Effect of contact time

Figure 6 shows the effect of contact time on the uptake rate of cadmium and lead ions by NaMOS. For initial metal concentrations of 2.225 $\times 10^{-4}$ and 2.415 $\times 10^{-4}$ mol L^{-1} for Cd(II) and Pb(II), respectively, the results revealed that for both metal ions, a rather fast adsorption of the cadmium ions occurs during the first 15 minutes, whereas for Pb(II), the process is marked by a slower process until equilibrium was reached. The rate of the metal ions sorption onto NaMOS is remarkably high. Typically, for both Cd(II) and Pb(II), up to 95% of the adsorption takes place within the first 15 min of contact time. Therefore, 60 minutes of contact time were enough for the sorption equilibrium to be achieved. This quite fast adsorption indicates the presence of abundant readily accessible adsorption sites, suggesting also that the removal process is very likely driven by

strong ionic interactions between the negatively charged maleate groups anchored at the surface of NaMOS material and metal ions in solution.

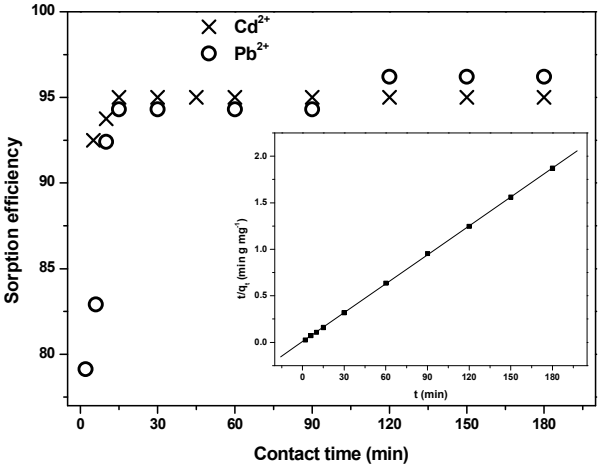

Figure 6. Effect of contact time on the uptake rate of Cd^{2+} and Pb^{2+} by NaMOS; inset: pseudo-second order plot for Pb^{2+} removal by NaMOS; adsorbent dose: 0.5 g L^{-1}; pH 5.

In contrast to the removal process of Cd(II) by NaMOS occurring in a short time, the slower sorption of Pb(II) was investigated by analyzing the kinetic data obtained from batch experiments using the pseudo-second order model given by Equation **(1):**

$$\frac{t}{q_t} = \frac{1}{k_2 q_e^2} + \frac{1}{q_e} t \qquad \textbf{(1)}$$

where k_2 is the rate constant of sorption (g mg^{-1} min^{-1}), q_e and q_t (mg g^{-1}) are the amounts of adsorbate uptaken at equilibrium and at time t, respectively.

A straight line was obtained when plotting t/qt versus t (Figure 6, inset). The equilibrium sorption capacity (q_e), the rate constant (k_2), and the coefficients (R^2) values were calculated from the linear plots. Perfect correlation is observed between experimental data and the pseudo-second order kinetic model with excellent correlation coefficients (higher than

0.999). The rate constant k_2 value was found to be 0.0135 g mg^{-1} min^{-1}. Additionally, the calculated q_e value (96.525 mg g^{-1}) from the model was totally in agreement with experimental sorption capacity, emphasizing therefore the accuracy of the model.

Sorption isotherms

The adsorption isotherms are displayed in Figure 7. The isotherms are characterized by a regular shape, with a steep initial slope, concave to the concentration axis. The high affinity of NaMOS adsorbent for the metal ions is suggested by the quantitative uptake at low adsorbate concentrations. The adsorption of cadmium and lead ions onto NaMOS increases with the initial metal ion concentration in reaching the equilibrium.

In order to understand the metal-adsorbent, the experimental data were analyzed by using the Langmuir and Freundlich isotherm models.

The linear form of Langmuir's isotherm model is given by the following equation:

$$\frac{C_e}{q_e} = \frac{C_e}{q_{max}} + \frac{1}{q_{max}\, b} \qquad (2)$$

where q_e (mg g^{-1}) is the actual amount of metal adsorbed, q_{max} (mg g^{-1}) is the maximum sorption capacity, C_e (mg L^{-1}) is the equilibrium concentration of metal in solution, and b (L mg^{-1}) is the Langmuir constant related to the energy of adsorption.

The Freundlich isotherm equation can be written in the linear form as:

$$log q_e = \frac{1}{n} log C_e + log k_F \qquad (3)$$

Where K_F (L g^{-1}) is the relative adsorption capacity constant of the adsorbent and $1/n$ is a constant related to the adsorption intensity.

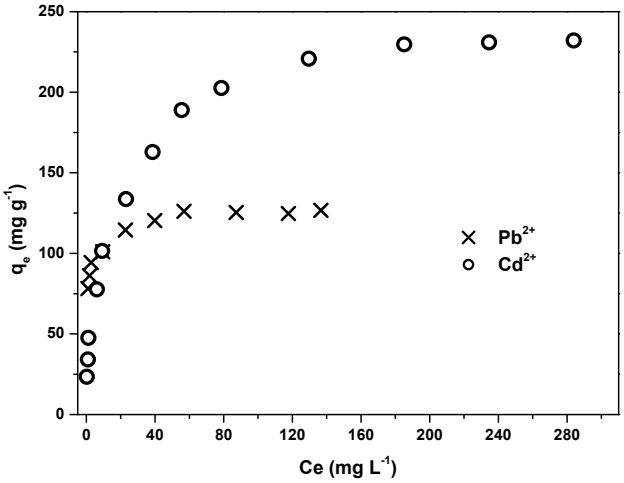

Figure 7. Adsorption isotherm for Cd^{2+} and Pb^{2+} onto NaMOS; adsorbent dose: 0.5 g L^{-1}; pH 5; contact time: 1h.

The analysis of the equilibrium experimental data of Cd(II) and Pb(II) adsorption onto NaMOS by using the Langmuir and Freundlich models showed that linear plots are obtained for both, as shown in Figures 8a and 8b, respectively. The linearized forms of both Langmuir and Freundlich equations were well fitted with the experimental data over a broad concentration range with excellent correlation coefficients values (Table 1).

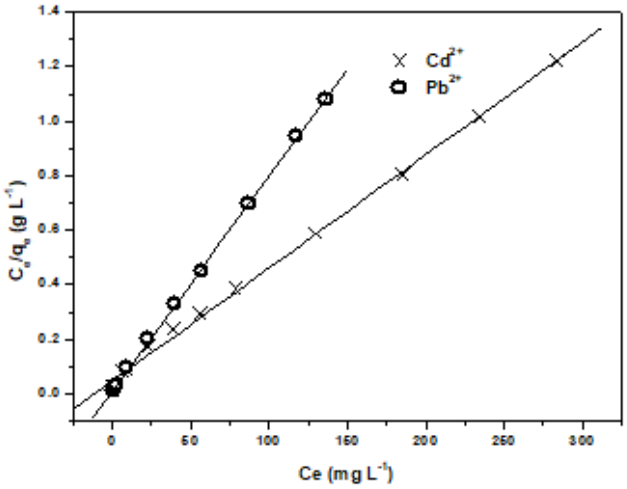

Figure 8.a. Langmuir plot for Cd^{2+} and Pb^{2+} removal by NaMOS.

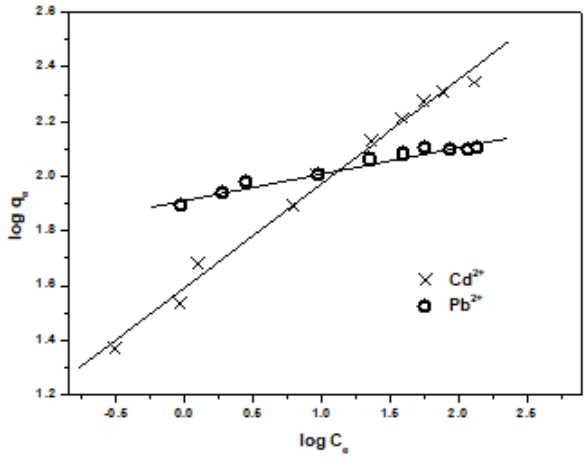

Figure 8.b. Freundlich plot for Cd^{2+} and Pb^{2+} removal by NaMOS.

These high adsorption capacities confirm the presence of abundant readily accessible adsorption sites and strongly suggest the homogeneous distribution of active carboxylate groups on the solid surface. However, as shown in Table 1, NaMOS had a preference for Cd(II) over Pb(II). The privileged affinity of NaMOS sorbent for Cd(II) is confirmed by the the values of the sorption capacities at saturation of the monolayer q_{max}, 240.96 mg g^{-1} Cd against 127.38 mg g^{-1}Pb. In molar units, the maximum sorption capacity of Cd(II) onto NaMOS was almost 3.5 times higher than that of Pb(II) (2.143 *vs*. 0.614 mmol g^{-1}). On the contrary, the affinity coefficient (*b*) of NaMOS was surprisingly higher for Pb(II) than for Cd(II), 0.672 L mg^{-1} *vs* 0.088 L mg^{-1}. The lower Pb(II) removal is for sure associated to the larger size of lead ion. Indeed, cadmium ions with their smaller hydrated radii[32-33] (1.03 Å) have easier access to the surface of NaMOS than the bulkier Pb(II) (1.32 Å). Therefore, the larger size of Pb(II) induces a quick saturation of adsorption sites, because of steric crowding and due to the virtual deficiency of other functional groups except carboxylate in MOS sorbent material, which may be involved in metal

uptake via cooperative mechanisms to stabilize the adsorption. These results suggest the homogeneous nature of NaMOS material and the availability of carboxylate groups at its surface. It also indicates that the ion-exchange process is the most appropriate mechanism involved in metal uptake.

Table 1. Langmuir and Freundlich isotherm constants for the sorption of Cd^{2+} and Pb^{2+} onto NaMOS.

	Langmuir constants			Freundlich constants		
Metal ion	q_{max} (mg g^{-1})	b (L mg^{-1})	R^2	K_F (L g^{-1})	$1/n$	R^2
Cd^{2+}	240.96	0.088	0.998	39.81	0.382	0.991
Pb^{2+}	127.38	0.672	0.999	81.28	0.096	0.964

The favorable adsorption of Cd(II) and Pb(II) onto NaMOS was also demonstrated by evaluating the separation factor R_L, defined by Weber and Chackravorti [34] and expressed by Equation (4):

$$R_L = \frac{1}{1+bC_0} \quad (4)$$

where b is the Langmuir constant, C_0 is the initial concentration and R_L indicates the shape of the isotherm ($RL > 1$ unfavorable; $RL = 1$ linear; $0 < RL < 1$ favorable; $RL < 0$ irreversible) . R_L values were determined for the whole concentration range and were between 0 and 1 in each case, indicating the favorable adsorption of Cd(II) and Pb(II) on NaMOS.

Figure 8b shows no deviation from linearity on the Freundlich plot for the whole concentration range. The Freundlich plots were also used to generate the intercept value of K_F and the slope $1/n$ (see Table 1).The capacity constant K_F and the affinity constant n are empirical constants dependent on several environmental factors[35]. The value of $1/n$ ranges between 0 and 1, indicating the degree of non-linearity between solution concentration and adsorption ($1/n > 1$, adsorption is a favorable physical process; $1/n = 1$, the adsorption is linear; $0 < 1/n < 1$, the adsorption process

is chemical; the more heterogeneous the surface is, the closer *1/n* value is to 0[36-38]. As shown in Table 1, the value of *1/n* is in the range of 0.096-0.382, confirming the favorized adsorption of Cd(II) and Pb(II) onto NaMOS.

Thermodynamic parameters

The removal of Cd(II) and Pb(II) by NaMOS adsorbent was studied at three temperatures values, in order to determine the thermodynamic parameters. The results are summarized in Table 2. The metal ion uptake decreased with an increase in temperature, indicating an exothermic process.

The thermodynamic parameters (ΔG^0, ΔH^0 and ΔS^0) were calculated by using the following equation:

$$logK_d = -\frac{\Delta G^0}{RT} = \frac{\Delta S^0}{R} - \frac{\Delta H^0}{RT} \quad (5)$$

where T is the temperature (K), R is the ideal gas constant (8.314 J $mol^{-1}K^{-1}$) and K_d is the distribution coefficient (amount of metal removed per gram of material divided by its concentration in the liquid phase).

The vant'Hoff plot of log K_d versus $1/T$ gave straight lines. The calculated slope and intercept from the plot were used to determine ΔH^0 and ΔS^0, respectively (see Table 2).

The negative value of ΔG^0 at each temperature indicates a favorable and spontaneous adsorption process and confirms the affinity of NaMOS material for Cd(II) and Pb(II). The negative value of ΔH^0 indicates that the adsorption is exothermic and also suggests that the adsorption process is a physical adsorption enhanced by chemical interactions between metal ions and maleate linkers through ion exchange. The positive value of ΔS^0 indicated the good affinity of the adsorbent for the metal ions and showed an overall increase of the degree of freedom in the system.

Table 2. Thermodynamic parameters for Cd^{2+} and Pb^{2+} removal by NaMOS adsorbent.

Metal ion	ΔH^0 (kJ mol^{-1})	ΔS^0 (J mol^{-1} K^{-1})	ΔG^0 (kJ mol^{-1})		
			20 °C	35 °C	45 °C
Cd^{2+}	–3.56	14.91	–7.99	–8.19	–8.34
Pb^{2+}	–0.96	23.86	–8.00	–8.31	–8.55

Desorption study

The desorption studies contribute to elucidate the nature of adsorption process and allow metal ions recovery as well as adsorbent regeneration for realistic applications in the treatment of industrial effluents. NaMOS can be readily regenerated with a molar aqueous solution of sodium chloride. Whereas brine solution has proven to be powerful for desorbing cadmium ions quantitatively from NaMOS (96–98%), excellent desorption performance for lead ions (85–92%) were however obtained under the same conditions over the three repeated adsorption–desorption cycles. As shown in Figure 9, while the third repeated use of the regenerated NaMOS material ended up with just a minor change in sorption effectiveness of cadmium ions (~ 7% loss), yet the first reusability of NaMOS for lead ions sorption, resulted in a dramatic decrease (ca. 12%) in its re-adsorption capacity. The adsorbent reusability for Pb(II) over three repeated cycles resulted in ca. 23% decrease in the material's capacity for lead sorption. In spite of this minor change, these results indicate that the chemically modified material can be fully regenerated while preserving exceptional performance for subsequent reuse.

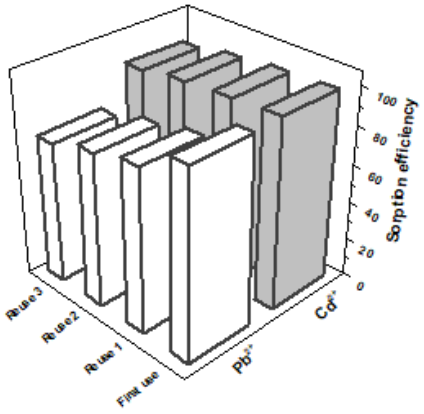

Figure 9. Removal efficiency of Cd^{2+} and Pb^{2+} by NaMOS sorbent over three adsorption–desorption cycles.

Experimental

Reagents and equipment

The raw material used in this study consisted of olive stone waste (HO-OS) supplied by ENCG factory, Sig, Algeria. The material was abundantly rinsed with tap water and finally with distilled water. The clean OS was then dried in an oven at 105°C until constant weight, before being ground and sieved to obtain particle sizes of 250 μm. All the chemicals used were of analytical reagents grade. Stock solutions of cadmium (II) and lead (II) were prepared by dissolving their nitrates in distilled water. The solutions were further diluted to the required concentrations before use. Infrared spectra were obtained on (2.5 wt %) samples in KBr disks from 500–4000 cm^{-1} using a Nicolet Avatar 330 Fourier transform IR spectrometer. Cross polarization magic angle spinning (CPMAS) ^{13}C NMR spectra of HO-OS and maleate-containing olive stone waste (MOS) were recorded on a Bruker 300 (Digital NMR Avance) spectrometer. The thermal stability of the samples was performed using thermogravimetric analysis

(TGA) and differential scanning calorimetry (DSC) on a NETZSCH STA 409 PC/PG simultaneous thermal analyzer. The specific surface areas were determined from the adsorption–desorption nitrogen isotherms at -196°C using a micrometrics ASAP 2020 apparatus. Before the analysis, the samples were degassed at 110°C for 24 h under vacuum. The surface area was calculated by applying the Brunauer–Emmett–Teller (BET) method from the linear part of the nitrogen adsorption isotherm.

Preparation of alkali olive stone waste NaO-OS

The chemical modification of olive stone waste (Figure 10) was carried out by immersing 100 g of clean olive stone waste (HO-OS) in 1000 mL of 20 wt.% aqueous sodium hydroxide solution. The resulting mixture was stirred for 4 hours at room temperature. The suspension was filtered and the solid was thoroughly washed with distilled water until neutral pH was obtained, and then washed with acetone. The material was then dried in an electric drying oven at 80°C and passed through a 250 μm sieve to obtain 58 g of NaO-OS as a brownish powder.

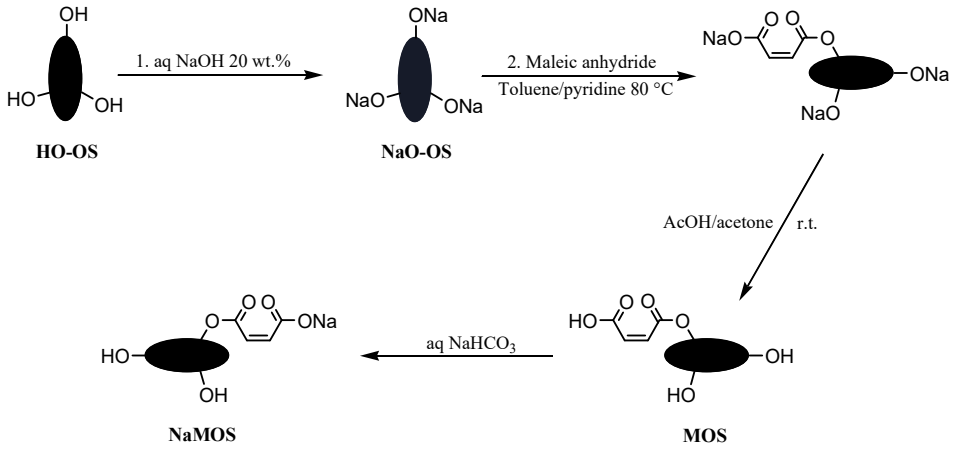

Figure 10. Synthesis of maleated olive stone MOS and its sodium salt (NaMOS).

Preparation of maleate-derived olive stone waste (MOS) and its sodium salt (NaMOS)

18 g of maleic anhydride was added to a suspension of soda olive stone waste NaO-OS (12 g) and pyridine (30 mL) in toluene (120 mL) heated at 60°C. The resulting mixture was left to stir for an hour at 80°C. After cooling to 60°C, the solid was filtered off and washed thoroughly with acetone to remove the unreacted maleic anhydride. The solid was then suspended in 100 mL of acetic acid solution (10 M) in acetone and left to stir for 2 h at room temperature. The solid was filtered, abundantly washed with distilled water, acetone and finally dried to yield MOS (16.72 g) as a yellowish solid which was sieved to a particle size of 250 μm.

NaMOS was prepared by the alkaline treatment of MOS with saturated sodium bicarbonate solution. The suspension was stirred at room temperature for 2 h and filtered. The solid was repeatedly washed with distilled water until neutral pH, then with acetone and finally dried and passed through 250 μm sieves.

Point of zero charge (pH_{PZC}) and CEC

The point of zero charge (pH_{pzc}) of the maleated olive stone waste (MOS) was measured using 0.01 M KNO_3 aqueous solutions at pH 2, 3, 4, 6, 8 and 10. These pH values were settled with either 0.1 M HCl or 0.1 M NaOH aqueous solutions. To 25 mL of each solution, 0.05 g of sample was added and the system was stirred for 24 h. The supernatant was then decanted and its pH was measured. The pHpzc value was obtained from a plot of initial solution's pH against pH of the supernatant.

The cationic exchange capacity of MOS material or the total content of carboxylic acid groups (n_{COOH}) was determined by standard back-

titration method[39-40]. 0.1 g of MOS sample was suspended in 100 mL of an aqueous 0.2 M NaOH solution and the resulting mixture was stirred for 2 h at room temperature. After filtration, the excess of NaOH was back-titrated with 0.2 M HCl using phenolphtaleine as indicator. The titration was triplicated and the average value of the HCl volume was used for the calculations. The amount of COOH (n_{COOH}) calculated from the obtained value of the equivalent volume of known HCl molarity according to the following equation:

$$n_{COOH} = V_{NaOH} \times C_{NaOH} - V_{HCl} \times C_{HCl}$$

Sorption experiments

The influence of pH was studied by contacting 25 mg of NaMOS adsorbent with 50 mL of solution at initial metal concentrations (25 mg L^{-1} Cd(II) and 50 mg L^{-1} Pb(II)) for 1 h. The initial pH was set between 4.0 and 6.0 by using solutions of HCl and NaOH. After 1 hour of agitation, the solution was filtered and the filtrate was analyzed by FAAS (Pye Unicam SP9 model). The sorbed amounts of cadmium and lead were determined from the difference between the initial and final concentrations by the following mass balance equation:

$$q_e = (C_i - C_e)V/W$$

where q_e is the amount (mg g^{-1}) of metal adsorbed, C_i and C_e are the initial and equilibrium metal ion concentrations (mg L^{-1}) in solution, respectively, V is the adsorbate volume (L) and W is the adsorbent weight (g).

The sorption isotherms were performed at pH 5 for both Cd(II) and Pb(II) with a solid/solution ratio of 0.5 g L^{-1}, at room temperature (20 ± 2°C). A fixed amount of adsorbent (25 mg of NaMOS) was dropped into 50 mL of metal solution with concentration varying between 10 and

400 mg L^{-1} for Cd(II) and 40-200 mg L^{-1} for Pb(II), then the suspension were maintained under agitation for 1 h. The suspensions were then filtered and the remaining concentrations of Cd(II) and Pb(II) were determined by FAAS.

Other adsorption experiments were also run to determine the equilibrium time (5-180 min) while reaching the maximum adsorption capacity with a fixed amount of adsorbent (25 mg of NaMOS) at initial metal concentrations of 25 mg L^{-1} for Cd(II) and 50 mg L^{-1} for Pb(II). Each experiment was carried out in triplicate and the average values are reported.

The influence of temperature on the removal process was studied for three different temperature values (20, 35 and 45 °C) at pH 5 on NaMOS suspensions in metal solutions at concentrations of 25 and 50 mg L^{-1} for Cd(II) and Pb(II), respectively. The solid/solution ratio was 0.5 g L^{-1}. The suspensions were stirred during 1h and then the metal concentration was analyzed by FAAS.

Desorption experiments

The regeneration was studied at pH 5 by contacting 100 mg of NaMOS adsorbent with 50 mL of metal solution (50 mg L^{-1} and 100 mg L^{-1} for Cd(II) and Pb(II), respectively) at room temperature for 1 h. After the adsorption experiment, NaMOS material was collected by filtration and washed thoroughly with distilled water to remove the excess metal ions, then it was suspended in 100 mL of 1M aqueous NaCl desorbing solution. The mixture was stirred for 1 h, filtered and the supernatant analyzed by FAAS. The regenerated material was abundantly rinsed with distilled water, then suspended in metal solution under the same conditions as above. The sorption-desorption cycles were repeated three times. The experiment was

carried out in duplicate to avoid any discrepancy in experimental results. The percentage of desorption (Dp) of Cd (II) and Pb(II) ions was calculated from the following expression, $D_p = 100\ (m_r/m_0)$, where m_r is the amount of metal ions desorbed (mg) and m_0 is the amount of metal ions adsorbed (mg).

Conclusions

In the present study, olive stone waste was converted into an added value adsorbent bearing maleate groups on its surface. This was accomplished by alkaline pretreatment of the raw olive stone waste for more effective esterification with maleic anhydride. The material was used to remove cadmium and lead ions from aqueous solution at an optimum pH of 5 using batch sorption experiments. Based on experimental data drawn from kinetics, pH effect, sorption capacities and carboxylate groups content, this work demonstrated that the chemically modified adsorbent performs efficiently through an uniform and fast sorption process with a pronounced affinity towards Cd^{2+} than Pb^{2+}. The removal process is exclusively connected to maleate linkers at the surface of the sorbent. In addition, Langmuir and Freundlich models adequately fitted the experimental data of cadmium and lead sorption onto NaMOS. Finally, the repeated use of the regenerated material ended up in just a minor change in sorption effectiveness. These results demonstrate that NaMOS adsorbent derived from olive stone waste is a promising material with high potential for the removal of heavy metal ions from aqueous solutions.

References

1. Gupta, V.K.; Rastogi, A. Biosorption of lead from aqueous solutions by green algae Spirogyra species: kinetics and equilibrium studies. *J. Hazard. Mater.* **2008**, *152*, 407–414.

2. Gupta, V.K.; Ali, I. Removal of lead and chromium from wastewater using bagasse fly ash – a sugar industry waste. *J. Colloid Interface Sci.* **2004**, *271*, 321–328.

3. Liu, D.H.F.; Liptack, B.G., Bouis, P.A. *Environmental Engineer's Handbook*, 2nd edn, Lewis, Boca Raton, FL, USA, 1997.

4. Hao, J.; Li, C.; Hu, C.; Wu, K. Rapid, efficient and economic removal of organic dyes and heavy metals from wastewater by zinc-induced in-situ reduction and precipitation of graphene oxide. *J. Taiwan Inst. Chem. Eng*. **2018**, *88*, 137-145.

5. Reddy, B.R., Priya, D.N. Chloride leaching and solvent extraction of cadmium, cobalt and nickel from spent nickel–cadmium, batteries using Cyanex 923 and 272. *J. Power Sources*, **2006**, *161*, 1428–1434.

6. Malla, M.E.; Alvarez, M.B., Batistoni, D.A. Evaluation of sorption and desorption characteristics of cadmium, lead and zinc on Amberlite IRC-718 iminodiacetate chelating ion exchanger. *Talanta,* **2002**, *57*, 277–287.

7. Navarro, R.; Saucedo, I.; Nunez, A.; Avila, M., Guibal, E. Cadmium extraction from hydrochloric acid solutions using Amberlite XAD-7 impregnated with Cyanex 921 (tri-octyl phosphine oxide). *React. Funct. Polym.* **2008**, *68*, 557–571.

8. Dabrowski, A.; Hubicki, Z.; Podkoscielny, P., Robens, E. Selective removal of the heavy metal ions from waters and industrial wastewaters by ion-exchange method. *Chemosphere* **2004**, *56*, 91–106.

9. El-Gohary, F.; Tawfik, A., Mahmoud, U. Comparative study between chemical coagulation/precipitation (C/P) versus coagulation/dissolved air flotation (C/DAF) for pre-treatment of personal care products (PCPs) wastewater. *Desalination* **2010**, *252*, 106–112.

10. Dubois, M.A.; Dozol, J.F.; Nicotra, C.; Serose, J., Massiani, C. Pyrolysis and incineration of cationic and anionic ion-exchange resins—Identification of volatile degradation compounds. *J. Anal. Appl. Pyrol.* **1995**, *31*, 129–140.

11. Reed, B.E.; Arunachalam, S.; Thomas, B. Removal of lead and cadmium from aqueous streams using granular activated carbon columns. *Environ. Program.* **1994**, *13*, 60–64.

12. Mohan, D.; Singh K.P. Single- and multi-component adsorption of cadmium and zinc using activated carbon derived from bagasse-an agricultural waste. *Water Research,* **2002**, *36*, 2304–2318.

13. Sigdel, A.; Jung, W.; Min, B.; Lee, M.; Choi, U.; Timmes, T.; Kimb, S-J. Concurrent removal of cadmium and benzene from aqueous solution by powdered activated carbon impregnated alginate beads. *Catena* **2016**, *148*, 101-107.

14. Çaglar, E.; Donar, Y.O.; Sinag, A., Birogul, I.; Bilge, S.; Aydincak, K.; Pliekhov, O. Adsorption of anionic and cationic dyes on biochars, produced by hydrothermal carbonization of waste biomass: effect of surface functionalization and ionic strength. *Turk. J. Chem*. **2018**, *42*, 86-99.

15. Faghihian, H.; Ghannadi, M.; Kazemian H. The use of clinptilolite of radioactive cesium and strontium from nuclear waste water and lead, nickel, cadmium, barium from municipal waste water. *Sep. Sci. Technol.* **1999**, *34*, 2275–2292.

16. Pansini, M.; Collella C. Dynamic data on lead uptake from water by chabazite. *Desalination* **1990**, *78*, 287–295.

17. Liu, H.; Peng, S.; Shu, L.; Chen, T.; Bao, T.; Frost, R.L. Magnetic zeolite NaA: Synthesis, characterization based on metakaolin and its application for the removal of Cu^{2+}, Pb^{2+}. *Chemosphere* **2013**, *91*, 1539–1546.

18. Srivastav, R.K.; Gupta, S.K.; Nigam, K.D.P.; Vasudevan, P. Use of aquatic plants for the removal of heavy metals from waste waters. *Int. J. Environ. Stud.* **1993**, *45*, 43–50.

19. Khozhaenko, E.; Kovalev, V.; Podkorytova, E.; Khotimchenko, M. **)** Removal of the metal ions from aqueous solutions by nanoscaled low molecular pectin isolated from seagrass Phyllospadix iwatensis. *Sci. Total Environ*. **2016**, *565*, 913–921.

20. Tuzen, M.; Sahiner, S.; Hazer, B. Solid phase extraction of lead, cadmium and zinc on biodegradable polyhydroxybutyrate diethanol amine (PHB-DEA) polymer and their determination in water and food samples. *Food Chem.* **2016**, *210*, 115–120.

21. Rafatullah, M.; Sulaiman, O.; Hashim, R. Ahmad, A. Adsorption of copper (II), chromium (III), nickel (II) and lead (II) ions from aqueous solutions by meranti sawdust. *J. Hazard. Mater*. **2009**, *170*, 969–977.

22. Gupta, V.K.; Mohan, D.; Sharma, S. Removal of lead from wastewater using bagasse fly ash - a sugar industry waste material. *Sep. Sci. Technol*. **1998**, *33*, 1331–1343.

23. Akhtar, M.; Iqbal, S.; Kausar, A.; Bhanger, M.I.; Shaheen, M.A. An economically viable method for the removal of selected divalent metal ions from aqueous solutions using activated rice husk. *Colloids Surf. B: Biointerfaces*, **2010**, *75*, 149–155.

24. Vilardi, G.; Di Palma, L.; Verdone, N. Heavy metals adsorption by banana peels micro-powder: Equilibrium modeling by non-linear models, *Chin. J. Chem. Eng*. **2018**, *26*, 455-464.

25. Martín-Lara, M.A.; Hernáinz, F.; Calero, M.; Blázquez, G.; Tenorio, G. Surface chemistry evaluation of some solid wastes from olive-oil industry used for lead removal from aqueous solutions. *Biochem. Eng. J.* **2009**, *44*, 151–159.

26. Aziz, A.; Elandaloussi, E.H.; Belhalfaoui, B.; Ouali, M.S. de Ménorval, L-C. Efficiency of succinylated-olive stone biosorbent on the removal of cadmium ions from aqueous solutions. *Colloids Surf. B: Biointerfaces.* **2009**, *73*,192–198.

27. Fiol, N.; Villaescusa, I.; Martínez, M.; Miralles, N.; Poch, J.; Serarols, J. Sorption of Pb(II), Ni(II), Cu(II) and Cd(II) from aqueous solution by olive stone waste. *Sep. Purif. Technol.* **2006**, *50*, 132–140.

28. Blázquez, G.; Hernáinz, F.; Calero, M.; Ruiz-Núñez, L.F. Removal of cadmium ions with olive stones: the effect of some parameters. *Process Biochem.* **2005**, *40*, 2649–2654.

29. Chang, S.; Chang, H. Comparisons of the photostability of esterified wood. *Polym. Degrad. Stabil.* **2001**, *71*, 261–266.

30. Liu, C.-F.; Sun, R.-C.; Qin, M.-H.; Zhang, A.-P.; Ren, J.-L.; Xu, F.; Ye, J.; Wu, S.-B. Chemical modification of ultrasound-pretreated sugarcane bagasse with maleic anhydride. *Ind. Crops Prod.* **2007**, *26*, 212–219.

31. Belhalfaoui, B.; Aziz, A.; Elandaloussi, E.H.; Ouali, M.S. and de Ménorval, L-C. Succinate-bonded cellulose: a regenerable and powerful sorbent for cadmium-removal from spiked high hardness groundwater. *J. Hazard. Mater.* **2009**, *169*, 831–837.

32. Emsley, J. *The Elements*. Clarendon Press, Oxford, USA, **1989**.

33. Mohan, D.; Kumar, H.; Sarswat, A.; Alexandre-Franco, M.; Pittman Jr. C.U. Cadmium and lead remediation using magnetic oak wood and oak bark fast pyrolysis biochars. *Chem. Eng. J.* **2014**, *236*, 513–528.

34. Weber, T.W.; Chakravorti, R.K. Pore and solid diffusion models for fixed bed adsorbers. *Am. Institut. Chem. Eng. J.* **1974**, *20*, 228–238.

35. Renault, F.; Morin-Crini, N.; Gimbert, F.; Badot, P-M.; Crini, G. Cationized starch-based material as a new ion-exchanger adsorbent for the removal of C.I. Acid Blue 25 from aqueous solutions. *Bioresour. Technol.* **2008**, *99*, 7573–7586.

36. Al-Duri, B., Adsorption modeling and mass transfer, In: *Use of Adsorbents for the Removal of Pollutants from Wastewaters*; G. McKay, Ed.; CRC Press: 1996, pp. 133–173.

37. Tien, C., *Adsorption Calculations and Modeling*; Butterworth–Heinemann Series in Chemical Engineering, Boston, 1994.

38. Treybal, R.E. *Mass Transfer Operations*; McGraw-Hill, New York, 1987.

39. Gurgel, L.V.A.; Karnitz Junior, O.; Gil, R.P.F.; Gil, L.F. Adsorption of Cu(II), Cd(II), and Pb(II) from aqueous single metal solutions by cellulose and mercerized cellulose chemically modified with succinic anhydride. *Bioresour. Technol.* **2008**, *99*, 3077–3083.

40. Karnitz, O.; Gurgel, L.V.A.; Perin de Melo, J.C.; Botaro, V.R.; Melo, T.M.S.; Gil, R.P.F.; Gil, L.F. Adsorption of heavy metal ion from aqueous solution single metal solution by chemically modified sugarcane bagasse. *Bioresour. Technol.* **2007**, *98*, 1291–1297.